Synthesis, Pharmacology, and Molecular Modeling Studies of Semirigid, Nicotinic Agonists

James A. Waters,*† Charles E. Spivak,*‡ Mark Hermsmeier,§,# Janardan S. Yadav,§,∥ Rong F. Liang,§,⊥ and Tamara M. Gund*§

Laboratory of Bioorganic Chemistry, National Institute of Diabetes and Digestive and Kidney Diseases, Bethesda, Maryland 20205, Addiction Research Center, National Institute on Drug Abuse, Baltimore, Maryland 20892, Department of Pharmacology and Experimental Therapeutics, University of Maryland School of Medicine, Baltimore, Maryland 21201, and Department of Chemistry and Chemical Engineering, New Jersey Institute of Technology, Newark, New Jersey 07102.
Received April 13, 1987

Eight nicotinic agonists were synthesized, and their potencies were estimated by contracture of the frog rectus abdominis muscle. The most potent, 1-methyl-4-acetyl-1,2,3,6-tetrahydropyridine methiodide (**3b**), 50 times as potent as carbamylcholine, served as a template for the rest. Although all of the agonists could easily conform to the putative nicotinic pharmacophore, their potencies spanned a nearly 10 000-fold range. This pharmacophore, therefore, may be necessary but deficient. Computer-assisted molecular modeling studies helped to delineate additional factors that may contribute to potency. The factors are (1) the ground-state conformation, (2) superimposability of the hydrogen bond acceptor and the cationic head onto the template, (3) electrostatic potential at the cationic head and at the hydrogen bond acceptor site, and (4) the presence of a methyl group bonded to the carbon atom that bears the hydrogen bond acceptor. A new program, ARCHEM, was used to calculate and to visualize electrostatic potentials at the van der Waals surfaces of the agonists.

The minimum, essential structure that activates the nicotinic acetylcholine receptor of voluntary muscle is the tetramethylammonium ion. Two classes of accessory groups that may enhance potency exist: (1) those containing an aliphatic hydrocarbon chain and (2) those containing an atom with unshared electrons. The alkyltrimethylammonium compounds and decamethonium are examples of the former class, and acetylcholine and nicotine are examples of the latter class. Barlow[1] suggested that a hydrogen bond formed between the receptor and the atom bearing the unshared electrons (a carbonyl oxygen in most nicotinic agonists). Beers and Reich,[2] comparing semirigid agonists (cytisine and nicotine, chiefly) and some competitive antagonists, concluded that the center of positive charge and the hydrogen bond acceptor are disposed in a particular geometrical relationship characterized by the distance between them and (they implied) by the angle between the cationic center and the carbonyl bond. This idea was recently corroborated by Sheridan et al. using more extensive molecular modeling studies.[3] This formulation corresponds to the gauche conformation of acetylcholine, which most studies conclude is the most stable one (reviewed in ref 4). Indeed, a model of acetylcholine in this conformation has helped guide our efforts to produce semirigid analogues.

Our objective has been to synthesize a highly potent, totally rigid agonist with which to gauge the recognition site of the nicotinic receptor. Although this goal remains elusive, our attempts did lead us to a semirigid agonist, isoarecolone methiodide (**3b**, Figure 1). This compound, 50 times more potent than carbamylcholine, is one of the most potent, semirigid, nicotinic agonists tested at the frog neuromuscular junction.[5] The high potency of **3b** and its monocyclic structure make it an ideal model compound that invites modification. For the analogues discussed here, most of the modifications were isomorphic substitutions, in which the basic structure remained constant but the atoms and the bond types composing it were systematically changed.

Scheme I. Synthetic Scheme of Agonists 1a-4a

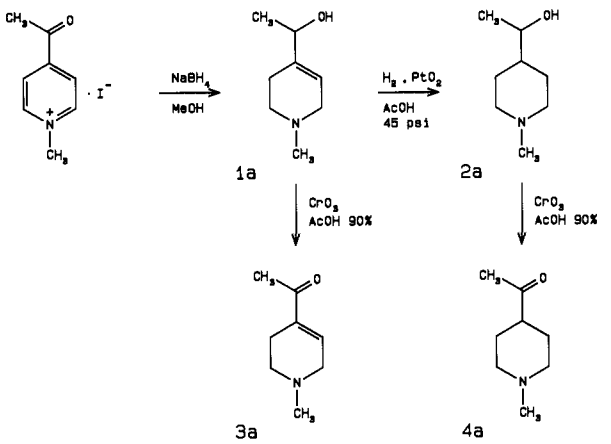

The major factors involved in receptor-ligand binding include structural and electrostatic properties of the receptor and of the ligands that bind to it. Three-dimensional modeling studies, which incude conformational analysis, electrostatic potential calculations, interactive computer graphics, and receptor mapping techniques can help to elucidate the structural and electrostatic requirements for agonist activity and provide a rational approach for design of new agonists with desired properties.[6]

In this paper we describe the synthesis and pharmacology of eight semirigid nicotinic agonists and attempt

† National Institute of Diabetes and Digestive and Kidney Diseases.
‡ National Institute on Drug Abuse and Department of Pharmacology and Experimental Therapeutics.
§ New Jersey Institute of Technology.
# Present address: The Squibb Institute for Medical Research, P.O. Box 4000, Princeton, NJ 08540.
∥ On leave of absence from Department of Physics, Banaras Hindu University, Varanasi 221005, U.P., India.
⊥ Present address: BASF Corp., 1255 Broad St., Clifton, NJ 07015.

(1) Barlow, R. B. *Introduction to Chemical Pharmacology*; Wiley: New York, 1955.
(2) Beers, W. H.; Reich, E. *Nature (London)* **1970**, *228*, 917.
(3) Sheridan, R. P.; Nilakantan, R.; Dixon, J. S.; Venkataraghavan, R. *J. Med. Chem.* **1986**, *29*, 899.
(4) Spivak, C. E.; Albuquerque, E. X. In *Progress in Cholinergic Biology: Model Cholinergic Synapses*; Hanin, I., Goldberg, A. M., Eds.; Raven: New York, 1982; p 323.
(5) Spivak, C. E.; Gund, T. M.; Liang, R. F.; Waters, J. A. *Eur. J. Pharmacol.* **1986**, *120*, 127.
(6) Review: Gund, T. M.; Gund, P. H. *Molecular Structures and Energetics, 4*; Liebman, J. F., Greenberg, A., Eds.; Verlag Chemie: Weinheim/Bergstr., Germany, 1986; p 319.

0022-2623/88/1831-0545$01.50/0

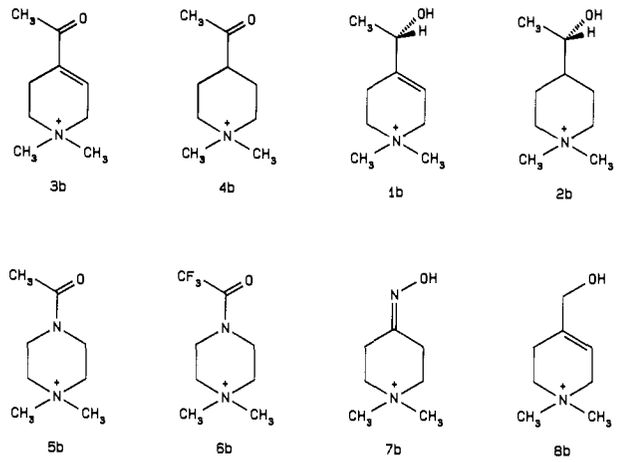

Figure 1. Nicotinic agonists: isoarecolone methiodide (**3b**), dihydroisoarecolone methiodide (**4b**), isoarecolol methiodide (**1b**), dihydroisoarecolol methiodide (**2b**), 1-methyl-4-acetylpiperazine methiodide (**5b**), 1-methyl-4-(trifluoroacetyl)piperazine methiodide (**6b**), 1-methyl-4-piperidone oxime methiodide (**7b**), 1-methyl-1,2,3,6-tetrahydropyridine-4-methanol methiodide (**8b**).

to correlate the measured potencies of these agonists with conformational and electrostatic results derived by use of the techniques of computer modeling. With this approach we hope to develop a rational model for design of new ligands.

Chemistry

The synthetic routes to piperidine compounds **1a,b–4a,b** are outlined in Scheme I. Sodium borohydride reduction of 1-methyl-4-acetylpyridinium iodide to 1-methyl-4-(2-hydroxyethyl)-1,2,3,6-tetrahydropyridine (**1a**) was carried out according to the procedure described by Lyle et al.[7] Hydrogenation to **2a** and oxidations to **3a** and **4a** were performed as shown in Scheme I. Free bases (**1a–4a**) are labile compounds requiring rapid conversions to the more stable methiodide salts (**1b–4b**). The free bases were stored under nitrogen at 0 to −35 °C for no longer than 18 h prior to their conversion to either the next intermediate or the methiodide salt. The synthesis of 1-methyl-4-acetylpiperazine methiodide (**5b**) has been described previously.[5] All attempts to purify 1-methyl-4-(trifluoroacetyl)piperazine methiodide (**6b**) by recrystallization caused decomposition. Analytical purity was achieved by quaternizing the tertiary precursor (**6a**), which had been purified by column chromatography.

Pharmacology. Equipotent molar ratios were estimated with isotonic contractures of the frog (*Rana pipiens*) rectus abdominis muscle with carbamylcholine as a standard. Three concentrations of the new agonist and three of the standard were administered in random order for an equal and fixed time, 2 min for drugs (**4b**, **1b**, **6b**, and **8b**) and 5 min for the weaker ones (**2b**, **7b**), exactly as described previously for **3b** and **5b**.[5] Aqueous solutions of **6b** lose some activity by around 1 h; therefore a working solution was prepared from a frozen stock solution about 2 min before each test.

The structures of the agonists are shown in Figure 1, and their potencies are given in Table I. Because **1b** and **2b** are racemic mixtures, the potencies of resolved enantiomers could be as much as 2 times greater than those given in Table I. Despite the structural similarities among these compounds, potencies ranged from 0.0055 to 50.0 times that of carbamylcholine.

Table I. Potencies of Nicotinic Agonists

compd	no. of frogs	potency[a,b]	95% confidence interval
3b	6	50.[c]	45.–56.
4b	7	9.1	8.0–10.4
1b	6	2.0	1.8–2.3
2b	5	0.25	0.21–0.30
5b	10	2.6[c]	2.4–2.8
6b	8	4.6	4.1–5.2
7b	6	0.0055	0.0046–0.0068
8b	6	0.35	0.30–0.42

[a] Potency is the reciprocal of the equipotent molar ratio compared to carbamylcholine. [b] Carbamylcholine produces one-half maximum depolarization of frog sartorius muscles at a concentration of abbout 25 M (Johnson, E. W.; Parsons, R. L. *Am. J. Physiol.* **1972**, *222*, 793. [c] From ref 5.

Computer-Assisted Molecular Modeling. Our objectives were to relate the differences in potencies to conformational and electrostatic properties of the agonists and to derive a model for binding to the nicotinic receptor. The overall approach used in these studies was first to derive minimum-energy conformations. From the minimum-energy conformations, a bioactive conformation was chosen on the basis of several criteria, as discussed below. The chosen bioactive conformations were then superimposed on isoarecolone methiodide (**3b**) as the template. Electrostatic contributions to potency were then evaluated for the chosen bioactive conformations.

Molecular modeling studies were performed with an Evans and Sutherland PS330 color vector/VAX 11/785 computer system and an AED 767/VAX 11/785 computer. Minimum-energy conformations were calculated by using a revised version of Allinger's[9] MM2 program, modified by Halgren[10] to handle formally charged molecules and parameterized for ammonium salts in collaboration with Snyder.[11] Amide parameters were obtained from Marshall.[12] The dihedral driver calculations were carried out by using the dihedral facility in MM2. The angle was rotated in 5-deg increments and then held constant while the remaining structure was geometry optimized. The molecules were superimposed, displayed and manipulated by using the SYBYL[13] and ChemX[14] programs. Partial changes were calculated by using Dewar's MNDO program from MOPAC.[15] The electrostatic potential (ESP) energies and their respective areas on the van der Waals surface were derived from the partial changes and a contouring program, ARCHEM.[16] The dielectric constant was set to 1. The points selected for ESP determination make a

(7) Lyle, R. E.; Perlowski, E. F.; Troscianiec, H. J.; Lyle, G. G. *J. Org. Chem.* **1951**, *20*, 1761.
(8) Huerta, P. L.; Isaacson, E. I.; Brown, R. G.; Delgado, J. N. *J. Pharm. Sci.* **1977**, *66*, 1120.
(9) (a) Burkert, U.; Allinger, N. L. *Molecular Mechanics*; ACS Monograph 177; American Chemical Society: Washington, DC, 1982; pp 1–319. (b) Allinger, N. L.; Yuh, Y. H. *Quantum Chemistry Program Exchange*, Prog. No. 395 (1980).
(10) Halgren, T. Merck, Sharp and Dohme Research Laboratories, unpublished.
(11) Snyder, J. Searle Pharmaceutical Co., Chicago, IL, and Gund, T., New Jersey Institute of Technology: ammonium parameters will be submitted to Dr. Norman Allinger for incorporation into the MM2 program; otherwise parameters can be obtained by writing to the authors.
(12) Marshall, G. Washington University, St. Louis, MO, private communication.
(13) Tripos Associates, St. Louis, MO 63117.
(14) Chemical Design Ltd., Oxford, U.K.
(15) Dewar, M. J. S. University of Texas, Houston, TX: MOPAC program available from the Quantum Chemistry Program Exchange.
(16) ARCHEM: Hermsmeier, M.; Gund, T. M., to be submitted to *J. Mol. Graphics.*

Table II. Preferred Conformations of Nicotinic Agonists

agonist	dihedral angle, deg	energy above global minimum, kcal/mol	Beers and Reich distance, Å
3b	−1	0.8	6.271
4b	15	1.3	6.213
1b	5	1.0	6.274
2b	20	1.7	6.162
5b	8	0.0	6.353
6b	7	0.0	6.313
7b	3	0.0	6.394
8b	−8	0.8	6.285

uniform distribution on the van der Waals surface. The atomic radii determine the extent of this surface. The areas of ESP ranges are determined by counting points within a range and multiplying by the area per point. This must be done separately for each atom type, since the area per point is slightly different for each atom type. The areas are very dependent on the atomic radii, which are as follows (Å): (C, sp^3 = 1.70; C, sp^2 = 1.74; O = 1.50; N = 1.60; H = 1.30; H, hydroxyl = 1.00; F = 1.45). Electrostatic potentials[17] were calculated in reference to an incoming, positive charge, and in this case, since the molecules have net positive charges, are calculated as repulsive energies.

Optimization Studies. Bioactive conformations were chosen by first considering all the conformers that fit the Beers and Reich[2] model for the nicotinic pharmacophore, namely those possessing a distance of 5.9 Å between the site of Coulombic interaction with the receptor (quaternary ammonium group) and the site of hydrogen bonding with the receptor (carbonyl oxygen or equivalent) at the van der Waals extension of oxygen. Compounds whose respective distances were between 5.5 and 6.4 Å were considered to fall within the Beers and Reich distance. Agonists with rotatable bonds were subjected to a dihedral driver calculation to derive all possible conformations resulting from bond rotations. All conformers fitting the Beers and Reich distance criterion and within 5 kcal of the lowest energy structure were candidates. Postulated bioactive conformations, which were used for superposition and other studies, are shown in Figure 2. Figure 3 gives a graph of dihedral angle versus energy calculated by the dihedral driver option of MM2 for the agonists with readily rotatable bonds (**1b**–**4b**, **8b**). Figure 4 relates derived dihedral angles to respective N···O distances (Beers and Reich criterion). Table II gives the numerical values of the preferred conformations in Figure 2.

We chose isoarecolone methiodide (**3b**) as the template molecule for superpositions because it is the most potent agonist, being 50 times more active than carbamylcholine.[5] Although the s-trans isomer of isoarecolone is 0.8 kcal lower in energy than the s-cis isomer (Figure 3), we chose the s-cis conformation as the bioactive form by analogy to other semirigid analogues, such as anatoxin *a*.[18–21] However, the models described here are actually independent of whether the s-cis or s-trans conformation is chosen as the bioactive species, since both fit the Beers and Reich model.

Superposition of Agonists. The agonists were superimposed four different ways, as indicated for **3b** in Figure 5. First the charged nitrogen and two adjacent carbons (Coulombic binding site, Figure 5a) were superimposed, and then the separation at the carbonyl or alcohol oxygens and adjacent sites was calculated. The second fit involved superposition at the carbonyl group and one of the ring carbons (C-2, Figure 5b) and then calculation of the separation at the ammonium and adjacent carbons. The third fit involved a superposition at the binding sites of the postulated pharmacophore, namely the charged nitrogen and the carbonyl group (Figure 5c), and then calculation of the fit at the carbonyl methyl and ring carbons. The fourth method superimposed the charged nitrogen, the carbonyl carbon atom, and the acetyl methyl group (Figure 5d), and then the fit at the remaining atoms was calculated.

Figures 6 and 7 show the superpositions of the agonists in Figure 2. Figure 6a shows the first superposition of isoarecolone methiodide (**3b**) (green), dihydroisoarecolone methiodide (**4b**) (red), isoarecolol methiodide (**1b**) (yellow), dihydroisoarecolol methiodide (**2b**) (blue), 1-methyl-4-acetylpiperazine methiodide (**5b**) (orange) and 1-methyl-4-(trifluoroacetyl)piperazine methiodide (**6b**) (magenta) at the ammonium nitrogen and two adjacent ring carbons. Whereas a perfect fit is obtained at the Coulombic regions (ammonium methyls and two adjacent methylenes), the hydrogen bonding regions do not align as well: the carbonyl oxygens as well as the acetyl methyls diverge by up to 2 Å compared to isoarecolone. If the fit of the cationic head and the carbonyl oxygen is critical, one may attempt to predict a rank order of potency by inspection of Figures 6 and 7: **3b** ~ **1b** ~ **8b** > **4b** > **2b** > **7b** > **5b** ~ **6b**. This rank order is far from the observed order, **3b** > **4b** > **6b** > **5b** > **1b** > **8b** > **2b** >> **7b**. In the same superposition, if one compares the deviation of the acetyl-like methyl from the template **3b**, one finds a much better prediction of rank order: **3b** > **4b** > **1b** > **5b** ~ **6b** > **2b**. Here is a suggestion that the position of this methyl group is important (evidence that its presence augments potency is discussed later). Figure 6b illustrates the second method of fitting of the same agonists, involving the carbonyl group, and the C-2 ring carbons. The importance of this ring position was suggested by the finding that unsaturation here always enhances potency (see Discussion). The predicted rank order of potency based on the fit of agonist N's to template N**3b** is **3b** ~ **1b** ~ **8b** ~ **2b** > **4b** > **5b** ~ **6b** ~ **7b**. Since the axial *N*-methyl may be important for activating the receptor,[4] we predict rank order by potency based on closeness of fit of these methyls to those of **3b**: **3b** ~ **1b** ~ **8b** > **4b** > **2b** > **5b** ~ **6b** ~ **7b**. Neither of these predicted rank orders is close to the observed one, suggesting that good superposition at this ring position is in itself unimportant. With the third, Beers and Reich fitting (ammonium nitrogen and carbonyl group, Figure 6c), the postulated pharmacophore groups are forced to fit. As Figure 6c shows, this superposition distinguishes the hydroxy- from the carbonyl-bearing agonists at the acetyl-like methyl group: a clear segregation appears. The rank order for closeness of fit to **3b** is **3b** ~ **4b** > **5b** ~ **6b** > **2b** > **1b**, which is similar to the observed order. Comparing axial *N*-methyl groups, one sees **3b** ~ **1b** ~ **8b** > **2b** ~ **4b** ~ **5b** ~ **6b** ~ **7b**. This second series is not very informative or useful. Figure 6d shows the fourth fitting, involving the ammonium nitrogen, the acetyl methyl, and the carbonyl carbon. Now one sees the oxygens diverging with rank order **3b** > **4b** > **6b** > **5b** ~ **7b**

(17) Politzer, P. *Chemical Applications of Atomic and Molecular Electrostatic Potentials*; Politzer, P., Truhbar, D. G., Eds.; Plenum: New York, 1981.
(18) Spivak, C. E.; Witkop, B.; Albuquerque, E. X. *Mol. Pharmacol.* 1980, *18*, 384.
(19) Koskinen, A. M. P.; Rapoport, H. *J. Med. Chem.* 1985, *28*, 1301.
(20) Gund, T.; Snyder, J. *Proceedings of the 8th International Symposium Medicinal Chemistry*, Upsala, Sweden, August 27–31, 1984.
(21) Spivak, C. E.; Waters, J.; Witkop, B.; Albuquerque, E. X. *Mol. Pharmacol.* 1983, *23*, 337.

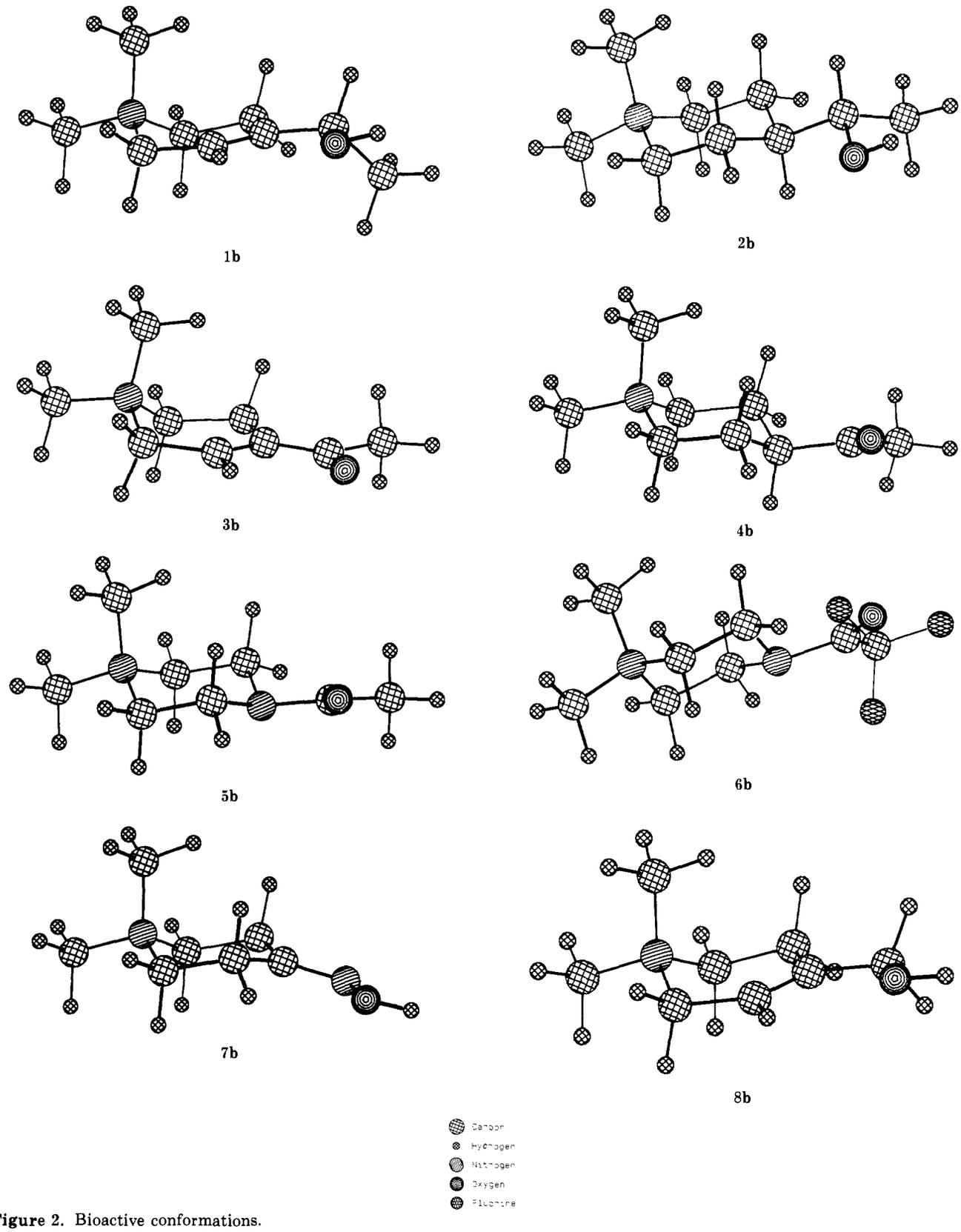

Figure 2. Bioactive conformations.

> **1b** ~ **8b** > **2b**. Except for the agonists without α-methyl groups (**7b** and **8b**), this is the rank order of observed potencies. The importance of the acetyl methyl group is also observed in the lowered potency of 1-methyl-3,4-dihydropiperidine-4-methanol (**8b**) relative to that of isoarecolol (**1b**). In superposition studies (Figure 7a,b) with isoarecolone methiodide (**3b**) (green), **8b** fits perfectly with the template, but the lack of a methyl group could be contributing to a lower potency. Figure 7a,b also illustrates the superposition of 1-methyl-4-acetylpiperazine methiodide (**5b**) (orange) and piperidone oxime methiodide (**7b**) (cyan) with the template **3b** (green) and the demethylated alcohol (**8b**). The oxime (**7b**) is another example of a demethylated agonist. It nearly superimposes on the acetylpiperazine (**5b**), but its low activity compared to that of **5b** indicates that this fit alone is insufficient. The

Table III. Areas (Square Angstroms) of Electrostatic Potentials on the van der Waals Surface

	energy range, kcal/mol						
agonist	0–40	40–60	60–80	80–100	100–120	120–140	140–160
3b	7.99	19.24	33.52	45.58	88.39	22.85	0.78
4b	7.46	17.14	39.16	63.69	84.52	18.37	0.00
1b	0.00	27.66	45.35	64.07	74.00	16.17	0.00
2b	0.00	30.74	45.91	68.06	77.36	14.79	0.00
5b	11.88	15.09	39.74	44.17	88.36	23.99	0.56
6b	17.74	34.58	18.45	35.56	94.49	34.48	2.36
7b	0.00	17.03	28.30	51.40	83.11	19.95	0.21
8b	0.00	11.93	36.32	66.12	75.26	16.85	0.00

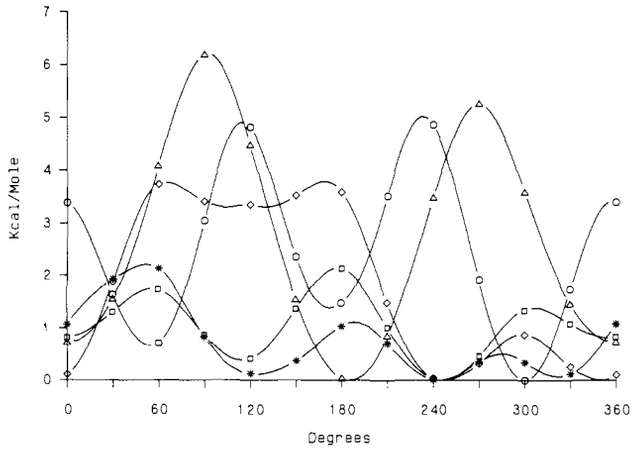

Figure 3. Energy vs dihedral angle for compounds **1b** (star), **2b** (circle), **3b** (triangle), **4b** (diamond), **8b** (square) (dihedral angles defined in Table II).

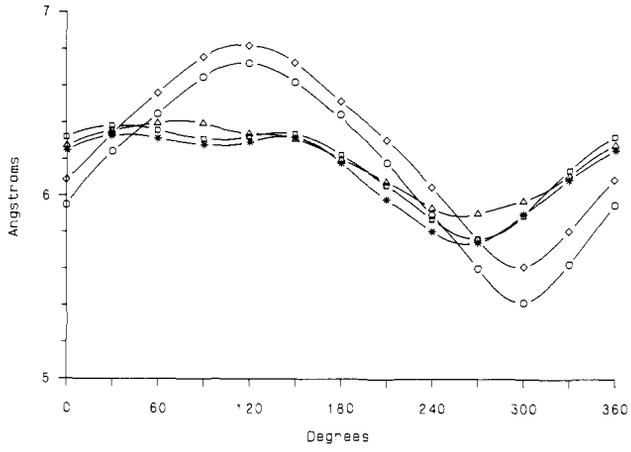

Figure 4. Distance from nitrogen to the van der Waals surface of oxygen vs dihedral angle for compounds **1b** (star), **2b** (circle), **3b** (triangle), **4b** (diamond), **8b** (square) (dihedral angles defined in Table II).

absence of a methyl group on the oxime could be important and could account in part for its lower activity.

In summary, close fit between a low-energy conformation of an agonist to the template is a factor that contributes to the activity of these agonists.

Electrostatic Potential Energy Calculations. Potential maps of the agonists in Figure 1 were derived with a newly developed program ARCHEM.[16] ARCHEM calculates the electrostatic potential at the van der Waals surface (or at other points, such as the solvent accessible surface at 1.2 Å beyond the van der Waals radius).

Figure 8 illustrates the electrostatic potential calculations on the van der Waals surfaces. The energies are color coded according to the range in electrostatic potentials. Table III gives the calculated values and the areas under each value in square angstrom units. The most positive

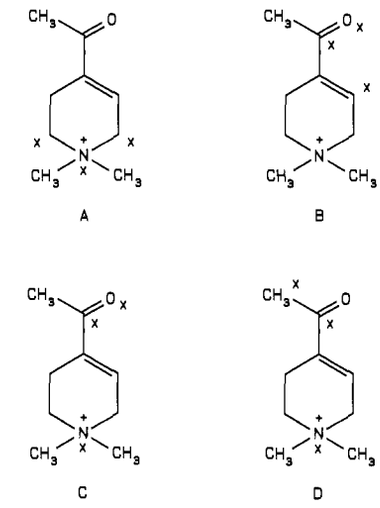

Figure 5. The four superposition sites: (A) Coulombic, (B) hydrogen bonding, (C) Coulombic and hydrogen bonding, (D) Coulombic and acetyl methyl.

areas, associated with the highest electrostatic potential energy (140–160 kcal), corresponds to the vicinity of the cationic head. The least positive areas, associated with the lowest electrostatic potential energy (0–40 kcal), correspond to the hydrogen bonding areas. We calculated the respective areas under each region (Figure 8) in an attempt to correlate the observed areas with potency. We observe that, in the most positive regions (140–160 kcal and 120–140 kcal), area of high electrostatic potentials decreased relative to **3b** with potency for all of the agonists except 1-(acetyltrifluoro)piperazine (**5b**). The finding that this agonist is more active than 1-(acetylmethyl)piperazine agrees with more positive electrostatic potentials around the Coulombic region. The regions of low electrostatic potentials are associated with the hydrogen bonding areas of the molecules. Some correlation with areas appears in that activity seems to drop off with area. For example, **6b**, which possesses a larger area of low electrostatic potential, is more active than **5b**. When one looks at the pictorial representation (Figure 8) one observes that not only is the area larger but the more negative area is spread to the methyl region. Again, evidence is accumulating that the methyl region is important for binding.

Discussion

The pharmacophore proposed by Beers and Reich (see ref 2 and 4) proved useful in guiding us to the highly potent agonist, isoarecolone methiodide,[5] **3b**. However, we wished to probe the receptor's sensitivity in discriminating among various agonists that, while bearing the requisite pharmacophore, presented it by different means. Four different types of hydrogen bond acceptors are represented: ketones, amides, alcohols, and an oxime. One expects a priori these chemical differences to be expressed as pharmacological differences, though we have little basis for pre-

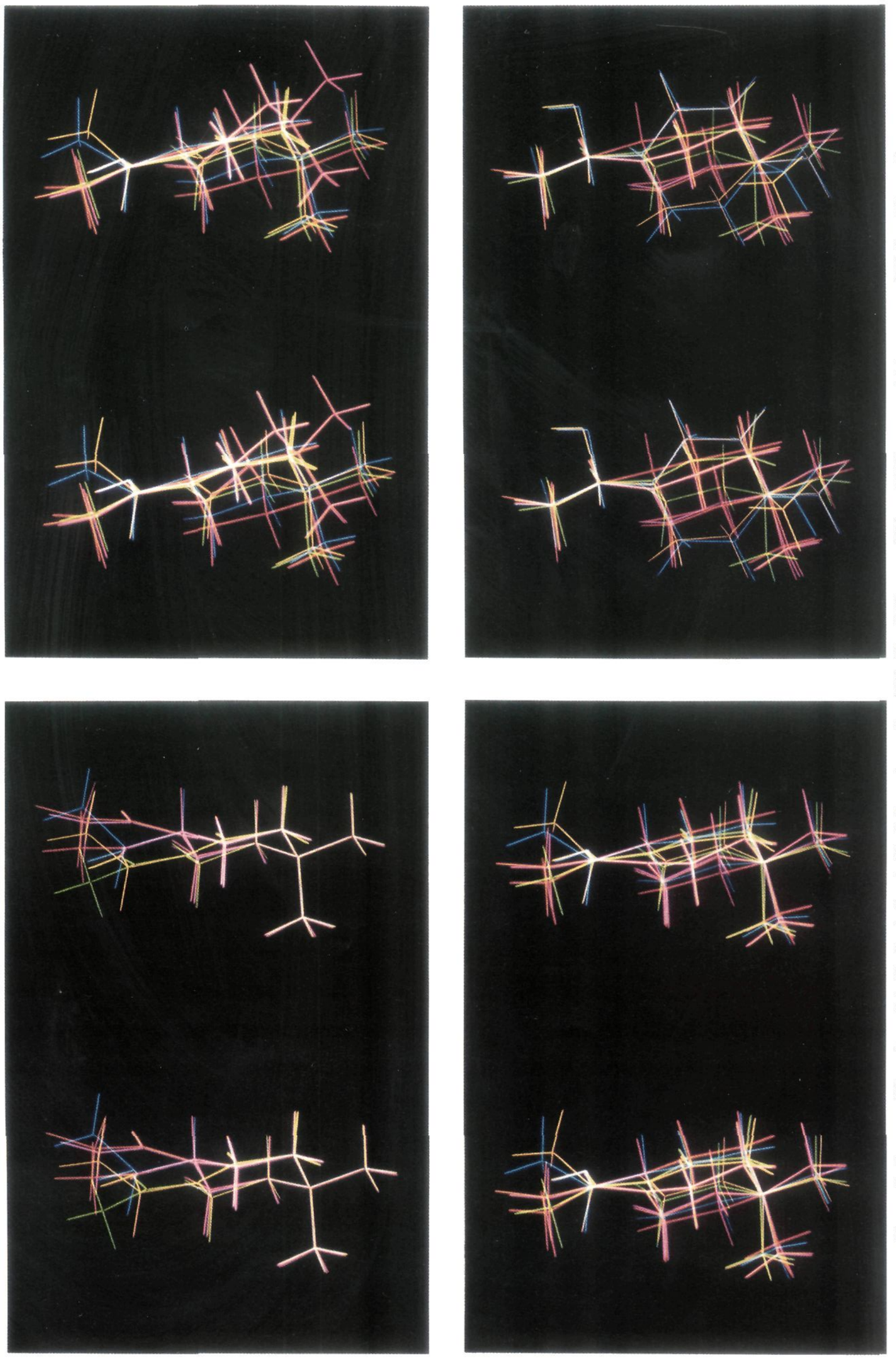

Figure 6. Superposition of agonists **1b–6b** at sites A–D. Color code: yellow (**1b**), blue (**2b**), green (**3b**), red (**4b**), orange (**5b**), magenta (**6b**) (see Figure 5).

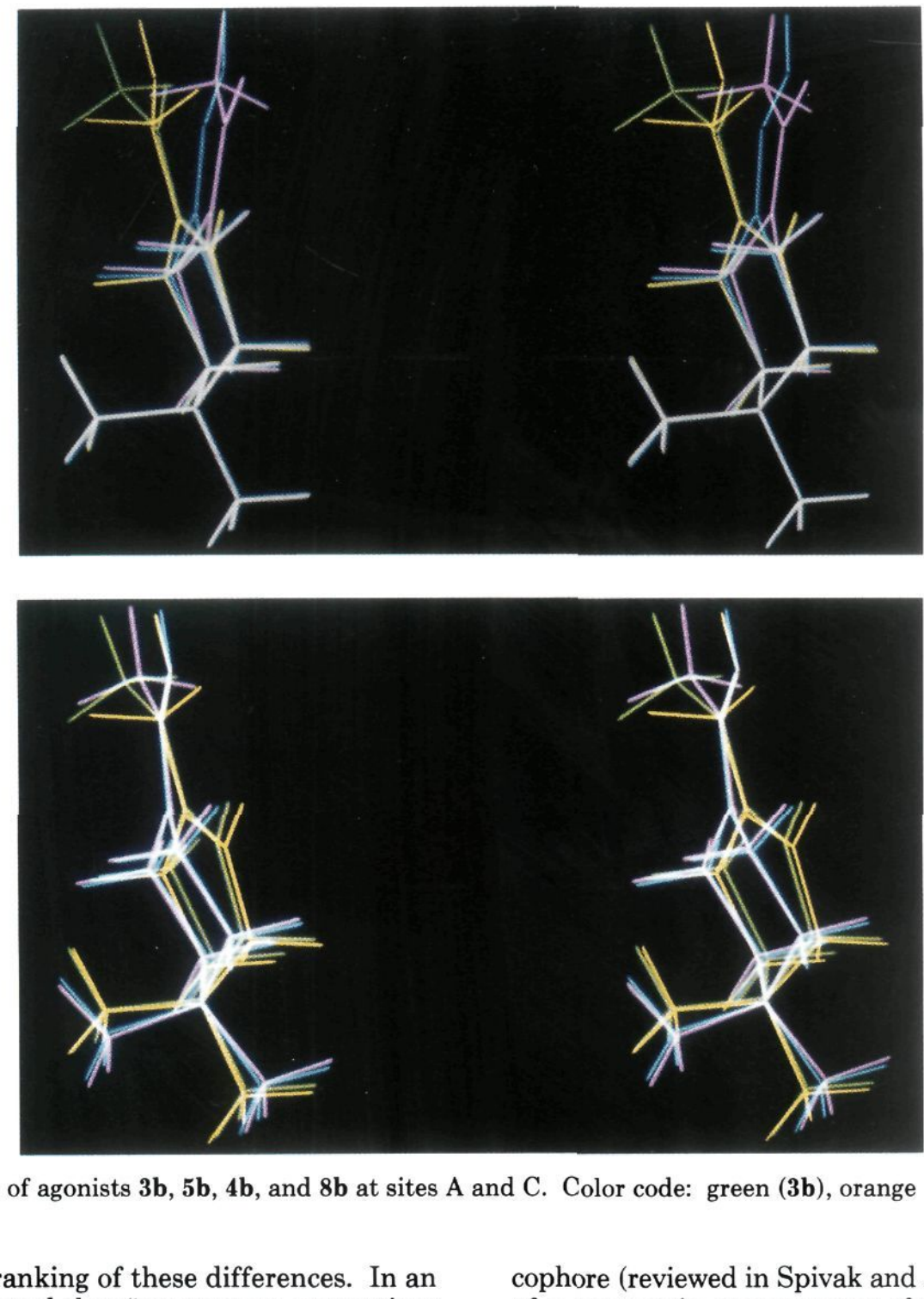

Figure 7. Superposition of agonists **3b**, **5b**, **4b**, and **8b** at sites A and C. Color code: green (**3b**), orange (**5b**), cyan (**7b**), yellow (**8b**) (see Figure 5).

dicting the range and ranking of these differences. In an early review, Riker[23] noted that "quaternary ammonium salts of the type $N^+Me_3A(OH)$, where A(OH) is a hydroxy substituted aliphatic chain, are among the weakest contracture-inducing substances in this general class of compounds". On this basis we expected that compounds **1b**, **2b**, and **8b** would be only marginally active.

This study represents an approach to rationalizing the structure of nicotinic agonists with potency. So many steps, some of which are still unknown, intervene between the desolvation that precedes the binding, through various obscure intermediate conformations of the receptor, to the final contracture of the muscle, that one cannot expect complete disentanglement of all the contributing factors. Some of these, the effects of structure on the kinetics of the ion channel governed by the nicotinic receptor, will be the subject of a later paper. The computer-assisted molecular modeling used in this paper provides plausible clues to activity of the eight agonists whose structures all appear to match that of the proposed pharmacophore, but whose activities span a nearly 10 000-fold range.

The fundamental assumption of most structure–activity studies is that there exists an optimal, static pharmacophore. Good ligands maximize coincidence with this pharmacophore while minimizing obstructive contacts with the receptor. Beers and Reich's[2] proposal for a pharmacophore (reviewed in Spivak and Albuquerque[4]) consisting of a geometric arrangement of the quaternary nitrogen atom and the carbonyl group has been corroborated recently by an independent, distance geometry method of Sheridan et al.[3] However, Table II shows that *all* of our agonists, potent and weak, can achieve this conformation with ambient thermal energy. As we discuss later, this *pharmacophore, while probably necessary for activity, is* incomplete. Additional factors may influence activity.

The double bond is seen in these agonists to enhance potency by 5.5 (compound **3b**:**4b**) or 8.0 (compound **1b**:**2b**), corresponding to a change in binding energy of 1.0 or 1.2 kcal/mol. In the similar enone, anatoxin *a*, the presence of the double bond enhances potency by a similar amount.[24] More than one mechanism may be operating. Our original view, still tenable, was that π-orbital overlap in the conjugated enone system populated a ground state identical with that of the pharmacophore.[18] Figure 3a confirms that the coplanar conformations (0° and 180°) lie in the two energy wells. Either of these conformations corresponds perfectly to the postulated pharmacophore depending on whether the nitrogen atom is flipped above or below the plane of the ring.

Though there is no conjugation in isoarecolol (**1b**), the conformations corresponding to the putative pharmacophore (at dihedral angles 0° and 180°) are over 1 kcal/mol

(22) Katritsky, A. R. *J. Chem. Soc.* **1955**, 2586.
(23) Riker, W. F., Jr. *Pharmacol. Rev.* **1953**, *5*, 1.
(24) Bates, H. A.; Rapoport, H. J. *J. Am. Chem. Soc.* **1979**, *101*, 1259.

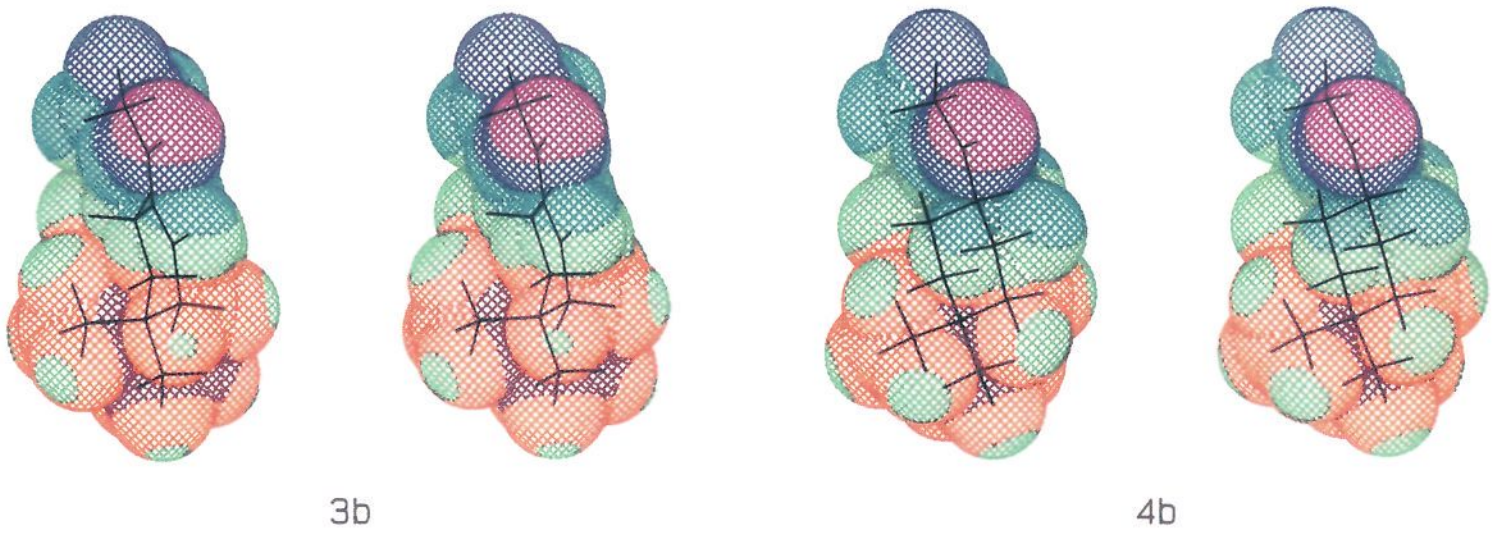

Figure 8. Stereo drawings of the electrostatic potentials on the van der Waals surface. Color code: purple (0–40 kcal), blue (40–60 kcal), turquoise (60–80 kcal), green (80–100 kcal), orange (100–120 kcal), brown (120–140 kcal), red (140–160 kcal).

above the global minimum (Figure 3a). At unrestrained equilibrium these conformations, while within easy reach, are virtually unpopulated. This could explain why isoarecolol (**1b**) is much less potent than isoarecolone (**3b**). By contrast, the dihydroisoarecolol (**2b**) has energy *maxima* of almost 5 kcal/mol at precisely the conformations of the pharmacophore (0° and 240°) due to simultaneous eclipsing of both the acetyl methyl group and the hydroxyl group with methylene groups in the ring. Its potency is therefore reduced further. All of this discussion of

ground-state conformation depends upon the assumption that rotation of the hydrogen bond acceptor into the conformation of the pharmacophore in the weaker agonists proceeds at a rate that is comparable to the rate-limiting step of binding.

Though the piperazines (**5b** and **6b**) have dihedral angles and electrostatic potentials appropriate for potent agonists (see below), the superpositions (Figures 6 and 7) show that a good fit with the template can only be obtained if the carbonyl oxygens are forced to fit. The stretching of the Coulombic or hydrogen bond attaching the agonist to the receptor is a plausible explanation for the reduced potencies of these compounds in comparison to **3b** and **4b**.

Further rationalization of potencies depends on considering the electrostatic potentials. Whereas on first sight the color-coded views of the agonists (Figure 8) appear similar, one must note that the differences between successive colors represents 20 (or more) kcal/mol, whereas we are seeking maximum differences in binding energy of only about 5 kcal/mol. Therefore subtle differences in these figures could be meaningful (Table III).

Since binding of the cationic head of the agonist to the receptor is Coulombic, we look at the potentials here first. Higher potential should tighten the bond. Ranking the homogeneous series **1b–4b**, we find **3b > 4b > 1b ~ 2b**. If we combine this series with the considerations of ground-state conformation above, we can rationalize the rank order in potency found. Comparing the two piperazines, we find **6b > 5b**, as one may expect given the electron-withdrawing effect of fluorine.

Hydrogen bonding to the agonist should be favored by high electron density at the acceptor site. Figure 8 and Table III show greater areas of low potentials on carbonyl oxygens than on hydroxyl oxygens (as expected from known group dipole moments). Potency is in keeping with this tendency. The oxime oxygen has the highest positive potential, which is in agreement with its being bonded directly to an electronegative atom. In addition, a resonance structure of the oxime leaves the oxygen electron deficient.

One more factor, not appreciated previously, that may disfavor the oxime is the absence of an acetyl-like methyl group. Evidence that this methyl group enhances activity is that 1-methyl-1,2,3,6-tetrahydropyridine-4-methanol methiodide (**8b**) is about one-seventh as active as the corresponding alcohol (**1b**) (Table I) despite the finding that the electrostatic picture is nearly identical with that of **1b** (Table III and Figure 8) and the conformational energies are very similar (Figure 3). The methyl group may enhance potency by one of several possible mechanisms: (1) by donating electron density to the hydrogen bond acceptor, (2) by occupying a specific site in the receptor, (3) by altering the solvation–desolvation balance that attends the binding of the agonist to the receptor, or (4) by directing the ground-state conformation of the agonist.

All of the explanations above could be considered speculative, but they do have predictive value. One could enhance potency of **3b** by substituting electron-withdrawing groups onto or into the ring. For example, the ring could be exchanged for a corresponding 1,3-oxazine system, or a ring hydrogen could be replaced by fluorine. Similarly, electron-withdrawing or -donating groups attached to the hydrogen bond acceptor, if they are not too bulky, may increase or decrease potency, respectively.

Conclusions

Computer-assisted molecular modeling has helped to identify various factors that may influence the activity of eight nicotinic agonists described here. All the agonists can easily assume the conformation of the proposed pharmacophore; indeed in the absence of modeling one would have limited means to rationalize potency. The factors that seem important are (1) ground-state conformation, (2) closeness of fit between the ground-state (or local minimum energy) conformation and the template agonist, **3b**, (3) high positive potential about the cationic head, (4) low potential about the hydrogen bonding acceptor, and (5) the presence of a methyl group adjoining the carbon atom bearing the hydrogen bond acceptor.

Experimental Section

Chemistry. Melting points were taken on a Kofler hot stage (corrected) or on a Fisher Johns melting point apparatus (uncorrected as noted). NMR spectra were recorded on a JOEL FX-100 or a Varian XL-300 spectrometer. CIMS were recorded on a Finnigan 1015 spectrometer. Infrared spectra were recorded on Perkin-Elmer 1330 or Beckman 4230 spectrophotometers. Elemental microanalyses were performed by Atlantic Microlab, Inc. (Atlanta, GA) and are within 0.4% of the theoretical values. Starting materials for syntheses were purchased from Aldrich Chemical Co. (Milwaukee, WI).

1-Methyl-4-(2-hydroxyethyl)-1,2,3,6-tetrahydropyridine Methiodide (Isoarecolol Methiodide, 1b). A brief description of the synthesis of the free base **1a** is given in ref 5. To a magnetically stirred solution of 1-methyl-4-acetylpyridinium iodide (2.32 g, 9.0 mmol) in 68 mL of N_2-purged MeOH, cooled to 5 °C in an ice bath, was added 1.50 g (40 mmol) of $NaBH_4$ portionwise over a period of 5 min. The reaction mixture was then removed from the ice and stirred at 21 °C for 30 min. H_2O (15 mL) was added and the mixture concentrated in vacuo at 50 °C to a thick slurry. Anhydrous K_2CO_3 was added with mixing and the resultant semisolid extracted eight times with 30-mL portions of Et_2O. The combined Et_2O extracts were dried ($MgSO_4$), and the solvent was removed in vacuo to yield 1.15 g of a clear, light tan oil. The crude product was column chromatographed on silica gel (230–400 mesh, 65 g). Elution with CH_2Cl_2–Et_2O (3:1) containing 3–12% of MeOH (N_2 purged) gave 1.03 g (81%) of 1-methyl-4-(2-hydroxyethyl)-1,2,3,6-tetrahydropyridine (**1a**), homogeneous by TLC [silica gel HLF; $CHCl_3$–MeOH–Et_2O (6:2:2)]. IR ($CHCl_3$): 3610 (OH), 1462, 1380, and 825 (CH=C) cm^{-1}. CIMS (NH_3): m/e 142 (M + 1).

To 24 mg of the secondary amino alcohol **1a** in 0.25 mL of acetone (filtered through a pledget of cotton) was added 0.02 mL of CH_3I. After the mixture was warmed for 2 h, the mother liquor was decanted from the tan solid. The solid was washed several times with cold acetone and then recrystallized from acetone–EtOH. The yield of methiodide salt **1b** as tan prisms was 24 mg, mp 187.5–188 °C. CIMS (NH_3): m/e 156 (M – I). ^1H NMR (D_2O): δ 5.63 (unresolv t, 1, 5 H), 4.78 (m, 2, C-6 CH_2), 4.71 (s, 1, OH), 4.34 (q, 1, C*H*(OH)CH_3), 3.98 (m, 2, C-2 CH_2), 3.49 (t, 2, C-3 CH_2), 3.11 (s, 6, $N(CH_3)_2$), 1.37 (d, 3, CH(OH)CH_3). Anal. ($C_9H_{18}INO$) C, H, N.

1-Methyl-4-(2-hydroxyethyl)piperidine Methiodide (Dihydroisoarecolol Methiodide, 2b). A solution of 500 mg (3.54 mmol) of 1-methyl-4-(2-hydroxyethyl)-1,2,3,6-tetrahydropyridine (**1a**) in 5 mL of glacial acetic acid containing 15 mg of PtO_2 was hydrogenated at 45 psi (21 °C) for 18 h with the Parr hydrogenator. After removal of the catalyst by filtration, the solvent was evaporated in vacuo (70 °C). To the semisolid was added 5 mL of H_2O saturated with NaCl, and then anhydrous K_2CO_3 was added with stirring. The resultant mixture was extracted five times with 15-mL portions of $CHCl_3$. The combined extracts were dried ($MgSO_4$), and the solvent was removed in vacuo to yield 395 mg of yellow oil. The crude **2a** was column chromatographed on 15 g of silica gel (230–400 mesh). Elution with $CHCl_3$–Et_2O (3:1) eluants containing 10–15% MeOH (N_2 purged) gave 87 mg (17%) of 1-methyl-4-(2-hydroxyethyl)piperidine (**2a**), homogeneous by TLC (silica gel GF, $CHCl_3$–MeOH–Et_2O (6:2:2). IR ($CHCl_3$): 3615 (OH), 1275, 1140, 1045, and 1010 cm^{-1}. CIMS (NH_3): m/e 144 (M + 1).

A portion (20 mg) of dihydro secondary alcohol **2a** was quaternized with CH_3I in the usual manner to give 35 mg of **2b** as a colorless solid, mp 174.5–175 °C, from acetone–EtOH. Anal. ($C_9H_{20}INO$) C, H, N.

1-Methyl-4-acetyl-1,2,3,6-tetrahydropyridine Methiodide (Isoarecolone Methiodide, 3b). A brief description of the synthesis of **3b** is presented in ref 5. To a stirred solution of 1.51 g (10.7 mmol) of 1-methyl-4-(2-hydroxyethyl)-1,2,3,6-tetrahydropyridine (**1a**) in 130 mL of glacial AcOH at 21 °C was added a solution of 790 mg of CrO_3 in 52 mL of 90% AcOH over a period of 25 min. After the reaction mixture stood for an additional 1.25 h, H_2O (15 mL) was added and the solution was washed with $CHCl_3$ (50 mL). The $CHCl_3$ layer was extracted with 5% $NaHCO_3$ and H_2O, and these aqueous extracts were added to the above H_2O layer. $NaHCO_3$ (12 g) was slowly added to the combined aqueous extracts with mixing. The solution was saturated with NaCl and extracted three times with 50-mL portions of $CHCl_3$. After the combined $CHCl_3$ extracts were dried ($MgSO_4$), they were evaporated in vacuo (50 °C) to yield 462 mg of brown oil. The crude product was column chromatographed on silica gel (18 g, 230–400 mesh). Elution with CH_2Cl_2–Et_2O (3:1) containing 2.0–3.5% MeOH (N_2 purged) gave 267 mg (18%) of isoarecolone (**3a**) as a reddish-brown oil, homogeneous by TLC (R_f 0.14, silica gel HLF, $CHCl_3$–MeOH–Et_2O, 6:2:2). IR ($CHCl_3$): 1668 (conj C=O), 1650 (inflection), 1620 (wk, conj C=C), 1452, 1425, 1372, and 1350 cm^{-1}. ^1H NMR (DMSO): δ 6.82 (unresolv, t, 1, 5-CH), 3.18 (d, 2, 6 CH_2), 2.98 (m, 2, C-2 CH_2), 2.57 (m, 2, C-3 CH_2), 2.42 (s, 6, $N(CH_3)_2$), 2.34 (s, 3, CH_3C=O).

The free base (**3a**) (207 mg) was immediately converted to the methiodide salt, yield 251 mg of light tan solid, as previously described. Recrystallization from acetone–EtOH (absolute) gave 210 mg of crystals, mp 177–178.5 °C. A second recrystallization from absolute EtOH gave the analytical sample **3b**, mp 177.5–178.5 °C. CIMS (NH_3): m/e 140 (M + 1 - CH_3I). ^1H NMR (D_2O): δ 6.93 (unrsolv t, 1, C-5 H), 4.75 (m, 2, C-6 CH_2), 4.18 (q, 2, C-2 CH_2), 3.54 (t, 2, C-3 CH_2), 3.14 (s, 6, $N(CH_3)_2$, 2.39 (s, 3, CH_3C=O). Anal. ($C_9H_{16}INO$) C, H, N.

1-Methyl-4-acetylpiperidine Methiodide (Dihydroisoarecolone Methiodide, 4b). A solution of 68 mg (0.48 mmol) of 1-methyl-4-(2-hydroxyethyl)piperidine (**2a**) in 6.5 mL of glacial AcOH was oxidized with 40 mg of CrO_3 in 2.5 mL of 90% AcOH as described above. The yield of crude dihydro ketone was 124 mg (oil). Column chromatography on silica gel (5 g, 230–400 mesh), with $CHCl_3$–Et_2O (3:1) eluants containing 3–12% MeOH (N_2 purged) gave 18.5 mg (27%) of pure 1-methyl-4-acetylpiperidine (**4a**) as a yellow oil that crystallized on standing. IR ($CHCl_3$): 3540 (C=O str overtone), 1720 (C=O) cm^{-1}. CIMS (NH_3): m/e 142 (M + 1).

The methiodide salt of the above ketone **4a** (18.5 mg) was prepared in the usual manner (reaction time 4 h). Crystallization of the reaction mixture took place at 0 °C. The yield of **4b** as pale yellow crystals was 6.4 mg, mp 188.5–190 °C. CIMS (NH_3): m/e 142 (M + 1 - CH_3I).

1-Methyl-4-(trifluoroacetyl)piperazine Methiodide (6b). To a cold solution of 1-methylpiperazine (0.9 g, 9.0 mmol) in 7 mL of acetone was added an excess of K_2CO_3. Trifluoroacetic anhydride (2.08 g, 9.9 mmol) in 4 mL of acetone was added dropwise with stirring to the above mixture. When the addition was complete, the mixture was warmed to 21 °C and stirred for an additional 20 min. The mixture was filtered and the solvent removed in vacuo. TLC (silica gel GF, acetone) showed the presence of five compounds, with the desired amide at R_f 0.41 (ca. 20%). The crude mixture was column chromatographed on silica gel (30 g, 60–200 mesh, 25-mL acetone fractions). The fifth fraction containing ca. 85% of **6a** was rechromatographed on 10 g of silica gel (acetone, 10-mL fractions). The sixth fraction contained highly pure **6a**. This free base was quaternized with CH_3I in the usual manner to yield 11 mg of **6b** as a colorless solid, mp 244–246 °C (uncorrected). IR (Nujol): 1710 cm^{-1}. Anal. ($C_8H_{14}F_3IN_2O$) C, H, N.

1-Methyl-4-piperidone oxime methiodide (7b) was prepared according to the procedure of Huerta et al.[8] The oxime **7a**, mp 127–129 °C (uncorr) (lit.[8] mp 128–129 °C) (1.0 g, 7.8 mmol) was quaternized with CH_3I in the usual manner (18-h reaction time) to yield 1.9 g (91%) of the oxime methiodide **7b** as colorless plates, mp 108.5–109.5 °C (uncorr), from H_2O–EtOH. IR (Nujol): 1650 (C=N) cm^{-1}. CIMS (NH_3): m/e 143 (M - I). Anal. ($C_7H_{15}IN_2O$) C, H, N.

1-Methyl-1,2,3,6-tetrahydropyridine-4-methanol Methiodide (8b). 4-Pyridiylcarbinol (5.0 g) in acetone (30 mL) was stirred with CH_3I (11.4 g) with cooling. After 30 min the precipitate (10.1 g) was filtered and washed with acetone and then Et_2O. The methiodide (2.0 g, 8 mmol) was dissolved in 15 mL of MeOH and $NaBH_4$ (0.98 g) was added in small portions with stirring. HCl (9 mmol) was then added to lower the pH to ca. 9. The solution was filtered (glass wool) and extracted four times with CH_2Cl_2 (50 mL). The extract was dried ($MgSO_4$) and the solvent was removed in vacuo to yield 0.93 g (92%) of colorless oil (**8a**). The free base was then dissolved in acetone (10 mL) and 2.3 g of CH_3I was added slowly. The product (1.1 g) was collected by filtration and recrystallized twice from EtOH–H_2O. A third recrystallization from acetone–H_2O gave the analytical sample **8b** as colorless needles, mp 182–183 °C (lit.[25] mp 176.5 °C). CIMS (NH_3): m/e 142 (M - I). Anal. ($C_8H_{16}INO$) C, H, N.

Acknowledgment. We are pleased to acknowledge the excellent technical assistance of Ba Ha (NIDDK). We thank the New Jersey Governors Commission on Science and Technology, The U.S. Army Medical Research Division, Fort Detrick, MD, Merck, Sharp and Dohme Laboratories, Rahway, NJ, Schering Plough Corp., Bloomfield, NJ, and Control Data Corp., for supporting this work. We also thank Tripos Associates for a grant of the SYBYL software and Chemical Design for a generous academic discount of the ChemX software.

(25) Ferles, M. *Chem. Listy* **1958**, *52*, 674; *Chem. Abstr.* **1960**, *52*, 13725c.